Average Peak Age of Information in Underwater Information Collection With Sleep-Scheduling

Article *in* IEEE Transactions on Vehicular Technology · May 2022

DOI: 10.1109/TVT.2022.3176819

5 authors, including:

Zhengru Fang
City University of Hong Kong
42 PUBLICATIONS **894** CITATIONS

SEE PROFILE

Jingjing Wang
Beihang University
240 PUBLICATIONS **8,220** CITATIONS

SEE PROFILE

Chunxiao Jiang
Tsinghua University
523 PUBLICATIONS **17,661** CITATIONS

SEE PROFILE

Average Peak Age of Information in Underwater Information Collection with Sleep-scheduling

Zhengru Fang, *Student Member, IEEE*, Jingjing Wang, *Senior Member, IEEE*, Chunxiao Jiang, *Senior Member, IEEE*, Xijun Wang, *Member, IEEE*, and Yong Ren, *Senior Member, IEEE*

***Abstract*—We investigate the peak age of information (PAoI) in underwater wireless sensor networks (UWSNs), where Internet of underwater things (IoUT) nodes transmit the latest packets to the sink node, which is in charge of adjusting the sleep-scheduling to match network demands. In order to reduce PAoI, we propose active queue management (AQM) policy of the IoUT node, beneficially compresses the packets having large waiting time. Moreover, we deduce the closed-form expressions of the average PAoI as well as the energy cost relying on probability generating function and matrix-geometric solutions. Numerical results verify that the IoUT node relying on the AQM policy has a lower PAoI and energy cost in comparison to those using non-AQM policy.**

***Index Terms*—Age of information, underwater wireless sensor networks, active queue management, multiple vacation queueing model.**

I. Introduction

With the emergence of Internet of underwater things (IoUT) in both civilian and military applications [1], [2], the metric of data timeliness has drawn substantially growing attention, since the timely update of sensing data is critical in monitoring systems, e.g., underwater target tracking, real-time sensing of currents and platforms, etc [3]. Therefore, age of information (AoI) is proposed to benchmark the timeliness of data in the face of the quality of experience (QoE), which is defined as the time elapsed since the last received status update packet is generated [4]. Besides, peak AoI (PAoI) can be utilized to evaluate a worse case of AoI, i.e., the maximum value of the age achieved before the latest update [5].

A range of studies have been carried out to minimise the AoI relying on queueing theory. Specifically, in [6], the average AoI and PAoI of different queueing models were investigated by considering GI/GI/1, M/G/1 and GI/M/1 queueing models[1]. In [7], Asvadi *et al*. studied the impact on PAoI of queueing models imposed by blocking and preemptive strategies, respectively. However, it is quite difficult to achieve timely underwater information collection without adaptive sampling and energy scheduling considering the hostile environment of underwater wireless sensor networks (UWSNs). Given that underwater sensors are battery-powered and costly to recharge, sleep-scheduling based on the vacation queueing model is necessary to apply to underwater sensors. As for AoI performance in UWSNs, Fang *et al.* in [3] proposed an autonomous underwater vehicle assisted underwater information collection scheme based on a limited-service M/G/1 vacation queueing system without work-sleep scheduling. In [8], Muhammad *et al*. proposed a traversal algorithm for underwater trajectory scheduling to improve the timeliness of data collected.

In this letter, we conduct an active queue management (AQM) scheme for IoUT information collection [9] to discard the low-timeliness packets relying on a multiple vacation M/M/1 queueing model. Furthermore, we derive the closed-form expressions of average PAoI in the context of both having AQM and non-AQM strategies in a first-in, first-out (FIFO) manner and infinite queue buffer, followed by a thorough analysis of IoUT node's energy cost. To the best of our knowledge, this is the first work that analyzes the PAoI performance of the multiple vacation queueing models.

The rest of this letter is organized as follows. Section II describes the network scenario, AoI metric and energy cost modelling. Then, the closed-form solutions of PAoI with different queue schedule policies are derived in Section III and IV, respectively. Numerical results are illustrated in Section V and Section VI concludes this letter.

II. Network Scenario and underwater acoustic channel model

A. Network Scenario

Without loss of generality, we consider a simple underwater environmental monitoring system consisting of N IoUT nodes and one sink node as shown in Fig. 1, where the IoUT nodes send the latest packets to the sink node by acoustic communication units. The packets are generated and stored at the IoUT nodes' queues in a FIFO manner. Each packet

This work was partly supported by National Natural Science Foundation of China (Grant No. 62071268 and 62127801), partly supported by the Young Elite Scientist Sponsorship Program by CAST (Grant No. 2020QNRC001), partly supported by Guangdong Basic and Applied Basic Research Foundation under grant 2021A1515012631, partly supported by the National Key R&D Program of China under Grant 2020YFD0901000. *(Corresponding author: Jingjing Wang.)*

Z. Fang and Y. Ren are with the Department of Electronic Engineering, Tsinghua University, Beijing, 100084, China. Y. Ren is also with Network and Communication Research Center, Peng Cheng Laboratory, Shenzhen 518055, China. E-mail: fangzhengru@gmail.com, reny@tsinghua.edu.cn.

J. Wang is with the School of Cyber Science and Technology, Beihang University, Beijing 100191, China. Email: drwangjj@buaa.edu.cn.

C. Jiang is with the Tsinghua Space Center, Tsinghua University, Beijing, 100084, China. E-mail: jchx@tsinghua.edu.cn.

X. Wang is with the School of Electronics and Information Technology, Sun Yat-sen University, Guangzhou 510006, China. E-mail: wangxijun@mail.sysu.edu.cn.

[1]Typically a queue can be described as three variables, i.e., A/S/K, where A and S denote the arrival and service process, respectively. K represents the number of servers. GI and G mean the general distribution, and M means that the interval of arrivals and service times yields exponential distribution.

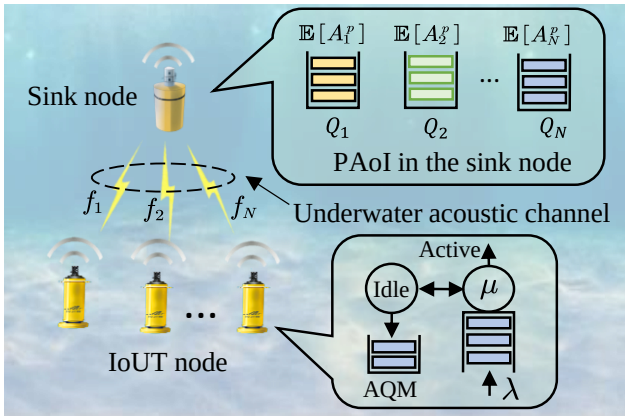

Fig. 1. Sleep-scheduling aided underwater information collection.

contains underwater environmental information and a timestamp recording the packet generation time. The generation of each packet follows a Poisson process with the arrival rate of λ. Besides, the service time of IoUT nodes is exponentially distributed with the rate μ. For the sake of both reducing AoI and saving energy, we assume that lossy packets are discarded without retransmission. Due to the limitation of batteries, it is impossible to keep uninterrupted transmission or follow a simple transmission mechanism, which may lead to excessive waste of energy. Therefore, the IoUT nodes should determine different modes, i.e., the active mode and the idle mode, according to dynamic workload state. Specifically, whenever the queue buffer of the IoUT node becomes empty, it switches to the idle mode. Moreover, in this mode, the IoUT node turns off the acoustic transmitter except in AQM procedure, while it still keeps data collection. If the queue keeps empty at the end of one idle period, the system continues to enter into another idle period, where the duration of one idle period is exponentially distributed with θ. Otherwise, the IoUT node switches to the active mode and transmits packets again. This sleep-scheduling based queueing system is modeled as the multiple vacation mechanism [10].

In the above scenario, we use a specific AQM for reducing average PAoI as well as network congestion in the idle mode. By using lossy techniques, the AQM is designed to compress and transmit the packets which have waited for a long time in idle mode. Specifically, lossy compression technique reduces bits by removing unnecessary or less important information. The launch of AQM obeys a Poisson process with the rate of γ. It is noted that IoUT node does not process compression if queue is empty. In the procedure of AQM, it processes packet in the head of the queue one after another, and compresses packet with a probability of α or keeps it with a probability of $\beta = 1-\alpha$, which is modeled as geometric abandonments [11]. Moreover, the AQM stops when the first packet is kept, or all packets are compressed and transmitted. After processing data compression, the compression ratio of data up to 55%-98%, where it saves energy cost up to 88%-97%. Thereby, relying on AQM policy, we ignore the energy cost of transmission during idle mode [12]. Considering the limited computational resource of IoUT node, we model the energy consumption of data compression in Section III.

B. The general definition of PAoI

In the considered scenario, we use PAoI to indicate the worse case of the packet AoI, which is influenced by packet generation rate, IoUT node transmit power and underwater channel delay. Furthermore, each IoUT node delivers packets by frequency-division multiple access (FDMA), and the sink node stores each packet in different storage locations according to its associated IoUT node. For simplicity, therefore, we only consider the i-th IoUT node's PAoI in the following section. Let α_n and β_n denote the packet generation time in the i-th IoUT node and received time in the sink node, respectively. n denotes the index of the status update. According to [6], the n-th average PAoI A_n^p is given by:

$$\mathbb{E}\left[A_n^p\right] = \mathbb{E}\left[\beta_n - \alpha_{n-1}\right] = \mathbb{E}\left[G_n\right] + \mathbb{E}\left[S_n\right], \tag{1}$$

where $G_n = \alpha_n - \alpha_{n-1}$ denotes the interval between the $(n-1)$-th and the n-th generated packets in the IoUT node. $S_n = D_n + \varrho_n$ represents the sum of system delay D_n and propagation latency ϱ_n. As the packet transmission for each IoUT node is independent of each other, the subscript "n" of the notations is omitted.

C. Underwater acoustic channel model

In this subsection, we analyze the network capacity of underwater acoustic communication channel in terms of transmit power, carrier frequency and aquatic environmental factors. Furthermore, the propagation latency ϱ of the underwater channel can be modeled as distance function. The attenuation of the channel over a distance l for the subchannel carrier frequency f is formulated as:

$$10\log\left[A\left(l,f\right)/A_0\right] = k\cdot 10\log l + l\cdot\log a\left(f\right), \tag{2}$$

where A_0 denotes a unit-normalizing constant, k represents the spreading factor, and $a(f)$ is the absorption coefficient. The first term of (2) denotes the spreading loss, while the second term represents the absorption loss. By using Thorp's model in [3], the absorption coefficient in dB/km for several kilohertz is formulated as:

$$10\log a(f) = \frac{0.11f^2}{1+f^2} + \frac{44f^2}{4100+f^2} + 2.75\cdot 10^{-4}f^2 + 0.003. \tag{3}$$

The ambient noise of underwater acoustic channel $N(f)$ can be formulated as the sum of four sources' power spectral density, i.e. turbulence $N_{\mathrm{t}}(f)$, shipping $N_{\mathrm{s}}(f)$, waves $N_{\mathrm{w}}(f)$ and thermal noise $N_{\mathrm{th}}(f)$. Therefore, the signal-to-noise ratio (SNR) for the IoUT node considered can be given by:

$$C(l,f) = B\log_2\left[1 + \frac{\eta P_{tr}\zeta(l,f)}{2\pi H\cdot(1\mu\mathrm{Pa})\cdot B}\right], \tag{4}$$

where η is the overall efficiency of circuit, the channel attenuation coefficient is $\zeta(l,f) = \left[A\left(l,f\right)N\left(f\right)\right]^{-1}$, and P_{tr} denotes the transmit power. H and B indicate the depth and sub-bandwidth of the IoUT node, respectively. Since the sink node only transmits packets at the active mode, we define $\mathbb{E}[\mathcal{E}]$ as the average energy cost of the active mode as follows:

$$\mathbb{E}[\mathcal{E}] = p_a P_{tr} T_t, \tag{5}$$

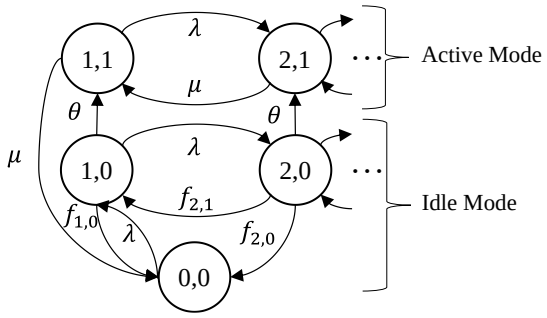

Fig. 2. The two-dimensional Markov chain of the AQM policy.

where p_a denotes the probability of the active mode in the IoUT node. T_t is defined as the average time from the existing packets being generated to departure from the IoUT node during the active mode. Additionally, the propagation latency of acoustic channel ϱ is formulated as $\varrho = \frac{l}{V_s}$, where V_s denotes the velocity of sound in water. For obtaining the closed-form expression of the average PAoI in Eq. (1), we derive the expectations of the interval of packet generation $\mathbb{E}[G_n]$ and the system delay $\mathbb{E}[D_n]$ in the following section.

III. PAoI of multiple vacation queue with AQM

In this section, we derive the average PAoI of multiple vacation queue relying on the AQM policy. According to the aforementioned assumptions, a continuous-time Markov chain models the considered system states as $\{N(t), J(t)\}$, which has a state space $\Theta = \{(0,0)\} \cup \{(k,j) : k \geqslant 1, j = 0, 1\}$. Let $N(t)$ and $J(t)$ denote the amount of packets and the mode of the IoUT node, respectively. $J(t) = 1$ represents the active mode, while $J(t) = 0$ denotes the idle mode. Then, we utilize $\boldsymbol{Q}_A$ to describe the instantaneous rate for the Markov chain state transition, and its element $q_{(i,j),(k,z)}$ denotes the departing rate from state (i,j) to (k,z). The diagram for the two-dimensional Markov chain based on vacation queueing model with AQM policy is portrayed in Fig. 2. Let $f_{i,j}$ denote the transition rate caused by AQM at idle mode. When $i \geqslant 1, j = 0$, we have $f_{i,j} = \gamma\alpha^{i+1}$, while $i > j > 0$, we have $f_{i,j} = \gamma\alpha^{i-j}\beta$, otherwise, $f_{i,j} = 0$. Therefore, the transition rate matrix $\boldsymbol{Q}_A$ can be formulated as:

$$\boldsymbol{Q}_A = \begin{pmatrix} \boldsymbol{B}_0 & \boldsymbol{C}_0 & & & & \\ \boldsymbol{B}_1 & \boldsymbol{A}_1 & \boldsymbol{A}_0 & & & \\ \boldsymbol{B}_2 & \boldsymbol{A}_2 & \boldsymbol{A}_1 & \boldsymbol{A}_0 & & \\ \boldsymbol{B}_2 & \boldsymbol{A}_3 & \boldsymbol{A}_2 & \boldsymbol{A}_1 & \boldsymbol{A}_0 & \\ \vdots & \vdots & \vdots & \vdots & \vdots & \ddots \end{pmatrix} \tag{6}$$

where $\boldsymbol{A}_0 = \mathrm{diag}(\lambda, \lambda)$, $\boldsymbol{C}_0 = (0, \lambda)$, $\boldsymbol{B}_0 = (\mu, \gamma\alpha)^{\mathsf{T}}$ and $\boldsymbol{B}_i = \left(0, \gamma\alpha^{i+1}\right)^{\mathsf{T}}$ with $i \geqslant 1$. Additionally, $\boldsymbol{A}_1 = \begin{pmatrix} -(\mu+\lambda) & 0 \\ \theta & -(\gamma\alpha+\theta+\lambda) \end{pmatrix}$, $\boldsymbol{A}_2 = \mathrm{diag}(\mu, \gamma\alpha\beta)$ and $\boldsymbol{A}_i = \mathrm{diag}(0, \gamma\alpha^{i+1}\beta)$ with $i \geqslant 3$. Because we only consider the behavior of the stable queue, the workload of queue yields $\rho = \lambda/\mu < 1$ for satisfying the balance condition (Theorem 1.7.1 in [13]). Then, the equilibrium distribution of the queueing system is defined as $\boldsymbol{\pi} = (\boldsymbol{\pi}_0, \boldsymbol{\pi}_1, \cdots)$, where $\boldsymbol{\pi}_i = \left(\pi_{i,1}, \pi_{i,0}\right)$, $(i \geq 0)$. The balancing equation is $\boldsymbol{\pi}\boldsymbol{Q}_A = 0$ and the normalization equation is $\boldsymbol{\pi}\boldsymbol{e} = 1$, in which $\boldsymbol{e} = (1, 1, \cdots)^{\mathsf{T}}$. Moreover, the partial PGFs of the active mode and the idle mode are $\Phi_a(z) = \sum_{n=0}^{\infty} \pi_{n,0} z^n$ and $\Phi_i(z) = \sum_{n=1}^{\infty} \pi_{n,1} z^n$, respectively. Substituting $\boldsymbol{Q}_A$ into the balancing equation, we can obtain the equilibrium distribution:

For active mode:

$$\pi_{n,1} = \begin{cases} 0, & n = 0, \\ \frac{\theta\pi_{1,0} + \mu\pi_{2,1}}{\mu+\lambda}, & n = 1, \\ \frac{\theta\pi_{n,0} + \lambda\pi_{n-1,0} + \mu\pi_{n+1,1}}{\mu+\lambda}, & n \geqslant 2. \end{cases} \tag{7}$$

For idle mode:

$$\pi_{n,0} = \begin{cases} \frac{\mu\pi_{1,1} + \gamma\sum_{i=0}^{\infty}\alpha^i\pi_{i,0}}{\lambda+\gamma}, & n = 0, \\ \frac{\lambda\pi_{n-1,0} + \gamma\beta\sum_{i=n}^{\infty}\alpha^{i-n}\pi_{i,0}}{\theta+\lambda+\gamma}, & n \geqslant 1. \end{cases} \tag{8}$$

Multiplying both sides of $\pi_{n,0}$ by z^n and summing for all $n \geq 1$, we can get the PGF for the idle mode:

$$\Phi_i(z) = \frac{(\theta+\lambda+\gamma)(z-\alpha)\pi_{0,0} - \gamma\beta z\Phi_a(\alpha)}{(z-\alpha)(\theta+\lambda+\gamma-\lambda z) - \gamma\beta z}, \tag{9}$$

where $z \neq \alpha$. Substituting $\pi_{0,0}$ into (9), we get $\Phi_i(\alpha) = \gamma^{-1}\left[(\lambda+\gamma)\pi_{0,0} - \mu\pi_{1,1}\right]$. Then, let $\Lambda_1(z)$ and $\Lambda_2(z)$ be the numerator and the denominator of $\Phi_i(z)$, respectively. Moreover, let z_0 be the root of $\Lambda_1(z)$. Let z_1 and z_2 be the roots of $\Lambda_2(z)$. Since $\Lambda_2(0) < 0$ and $\Lambda_2(1) > 0$, we have $0 < z_1 < 1 < z_2$. If the queue system is stable, $\Phi_i(z)$ is convergent with $|z| \leqslant 1$. Therefore, according to Rouché's theorem [13], we have $z_0 = z_1$, $\Lambda_1(z_1) = 0$ and $\Phi_i(z) = \frac{z_2}{z_2 - z}\pi_{0,0}$, where $z_1(z_2) = \frac{-\gamma\beta+\theta+\lambda+\gamma+\alpha\lambda-(+)\sqrt{\Delta}}{2\lambda}$ and $\Delta = [(\theta+\lambda+\gamma)+\alpha\lambda-\gamma\beta]^2 - 4\alpha\lambda(\theta+\lambda+\gamma)$. According to $\Lambda_1(z_1) = 0$ and $z_1 z_2 = \lambda^{-1}\alpha(\lambda+\theta+\gamma)$ and $z_1 + z_2 = \lambda^{-1}(\lambda+\lambda\alpha+\theta+\gamma\alpha)$, we can derive that $\pi_{1,1} = (\beta\mu)^{-1}[\lambda z_2 - (\theta+\alpha\lambda+\alpha\gamma)\pi_{0,0}]$. Likewise, we can derive $\Phi_a(z) = \frac{z\theta\Phi_i(z) - z\left[\theta\pi_{0,0} + \mu\pi_{1,1}\right]}{(\lambda z - \mu)(1-z)}$ by using the same steps above. Substituting $\pi_{1,1}$ and $\Phi_i(z)$ back to $\Phi_a(z)$, the PGF for the active mode can be expressed as:

$$\Phi_a(z) = \frac{z\pi_{0,0}z_2\left[\lambda(1-z_1)z - (\lambda z_2 - \lambda z_1 z_2 - \theta\beta)\right]}{\beta(z_2 - z)(\lambda z - \mu)(1-z)}. \tag{10}$$

According to Rouché's theorem [13], the numerator of $\Phi_a(z)$ has a root $z = 1$. Hence, we can obtain $\Phi_a(z) = \frac{z\pi_{0,0}z_2\lambda(1-z_1)}{\beta(z_2-z)(\mu-\lambda z)}$. Furthermore, the PGF of the equilibrium distribution $\boldsymbol{\pi}$ can be given by $\Phi(z) = \Phi_a(z) + \Phi_i(z)$. Thus, we obtain the probabilities of active mode $p_a = \Phi_a(1)$ and of idle mode $p_i = \Phi_i(1)$, respectively. Relying on the normalization equation $\Phi(1) = \boldsymbol{\pi}\boldsymbol{e} = 1$, the steady-state probability $\pi_{0,0}$ is formulated as:

$$\pi_{0,0} = \frac{\beta(z_2 - 1)(\mu - \lambda)}{z_2\left[\beta(\mu-\lambda) + \lambda(1-z_1)\right]}. \tag{11}$$

Taking derivative and substituting $z = 1$, the average queue length with AQM is derived as:

$$\mathbb{E}[L_A] = \Phi_i'(1) + \Phi_a'(1). \tag{12}$$

After some algebra, the average queue length in the IoUT node relying on the AQM policy is formulated as:

$$\mathbb{E}[L_A] = \frac{z_2\pi_{0,0}}{(1-z_2)^2} + \frac{\rho(1-z_1)z_2\pi_{0,0}(z_2-\rho)}{\beta(z_2 - \rho z_2 - 1 + \rho)^2}. \tag{13}$$

The packets arriving at the IoUT node follows the Poisson process with the arrival rate of λ. Therefore, the average inter-arrival time of packets is $\mathbb{E}[G] = \lambda^{-1}$. According to the Little's

law [10], $\mathbb{E}[D_A] = \lambda^{-1}\mathbb{E}[L_A]$. Assuming the stationary and i.i.d transmission process, we have $\mathbb{E}[G_n] = \mathbb{E}[G]$ and $\mathbb{E}[S_n] = \mathbb{E}[D_A] + \varrho$, where ϱ denotes the propagation latency delay in underwater acoustic channel. According to Eq. (1) and (13), the average PAoI of the packet generated in the receiver of the sink node yields:

$$\begin{aligned}\mathbb{E}\left[A_A^p\right] &= \mathbb{E}[G] + \mathbb{E}[D_A] + \varrho \\ &= \frac{1}{\lambda}\left[1 + \frac{z_2\pi_{0,0}}{(1-z_2)^2} + \frac{\rho(1-z_1)z_2\pi_{0,0}(z_2-\rho)}{\beta(z_2-\rho z_2-1+\rho)^2}\right] + \varrho.\end{aligned} \tag{14}$$

The energy cost is formulated as the average power consumption during the unit time T_t in the associated IoUT node. Relying on Eqs. (5) and (10), the energy cost of data transmission is obtained as follows:

$$\mathcal{E}_A^{tr} = p_a P_{tr} T_t = \frac{z\pi_{0,0}z_2\lambda(1-z_1)}{\beta(z_2-1)(\mu-\lambda)} P_{tr} T_t. \tag{15}$$

While the energy consumption for data compression by the IoUT node is given by

$$\mathcal{E}_A^c = (1-p_a)\kappa[\rho_c \lambda L]^3 T_t, \tag{16}$$

where κ and ρ_c denote the effective switched capacitance and the processing density, respectively. Relying on AQM policy, the sum of energy cost in the IoUT node can be formulated as $\mathcal{E}_A = \mathcal{E}_A^{tr} + \mathcal{E}_A^c$.

IV. PAoI of Multiple Vacation Queue with non-AQM

In this section, we derive the average PAoI for multiple vacation queue without AQM (i.e., non-AQM policy), i.e. the IoUT node does not compress and transmit outdated packets in its idle mode. Substituting $\beta = 1$ and $\alpha = 0$ (i.e., $f_{i,j} \equiv 0$.) back to Eq. (6), we achieve the transition rate matrix $\boldsymbol{Q}_{NA}$ for the system relying on non-AQM policy, and its status update is formulated as a quasi-birth-and-death (QBD) process. Since the system is ergodic, the probabilities $\boldsymbol{\pi}_i$ yield the recursive relationship, i.e., $\boldsymbol{\pi}_{i+1} = \boldsymbol{\pi}_i \boldsymbol{R}$ and $\boldsymbol{\pi}_k = \boldsymbol{\pi}_0 \boldsymbol{R}^k$ with $k \geq 0$. According to the matrix-geometric solutions in [13], the square matrix $\boldsymbol{R}$ is a nonnegative solution for the following matrix-quadratic equation:

$$\boldsymbol{R}^2\boldsymbol{D}_0 + \boldsymbol{R}\boldsymbol{A} + \boldsymbol{C} = \boldsymbol{0}, \tag{17}$$

where $\boldsymbol{D}_0 = \mathrm{diag}(\mu, 0)$, $\boldsymbol{A} = \begin{pmatrix} -(\mu+\lambda) & 0 \\ \theta & -(\theta+\lambda) \end{pmatrix}$, $\boldsymbol{C} = \mathrm{diag}(\lambda, \lambda)$ are lower triangular matrices. Then, we define $\boldsymbol{R} = \begin{pmatrix} r_{11} & 0 \\ r_{21} & r_{22} \end{pmatrix}$ as a lower triangular matrix accordingly. Substituting them back to (17), we obtain the equations about the elements of $\boldsymbol{R}$:

$$\begin{cases} \mu r_{11}^2 - (\mu+\lambda) r_{11} + \lambda = 0, \\ (r_{21}r_{11} + r_{22}r_{21})\mu - (\mu+\lambda) r_{21} + \theta r_{22} = 0, \\ \lambda - (\theta+\lambda) r_{22} = 0. \end{cases} \tag{18}$$

Thus, we find the minimal nonnegative solution as follows: $r_{11} = \rho$, $r_{22} = \lambda/(\theta+\lambda)$ and $r_{21} = \theta r_{22}/[\mu(1-r_{22})]$, where $\rho = \lambda/\mu$ denotes the workload of the queue. Relying on the normalization condition $\boldsymbol{\pi}_0(\boldsymbol{I}-\boldsymbol{R})^{-1}\boldsymbol{e} = 1$ [13], we can get $\boldsymbol{\pi}_0$. Furthermore, the probability of the active mode in the IoUT node relying on non-AQM policy is formulated as:

$$p_{NA,a} = \sum_{k=1}^{\infty} \pi_{k,1} = \frac{r_{21}}{1-\rho+r_{21}}. \tag{19}$$

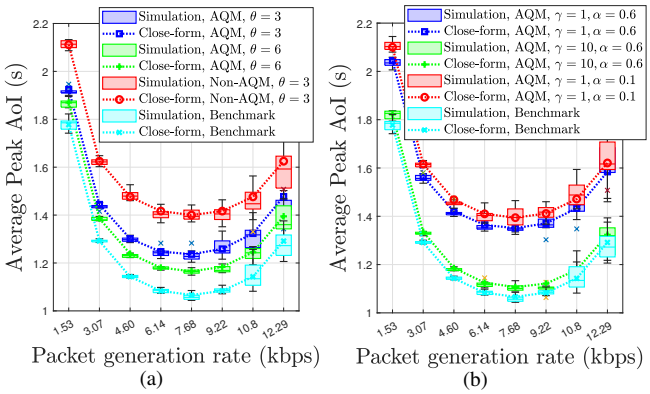

Fig. 3. The average PAoI under three policies over different packet generation rate λI

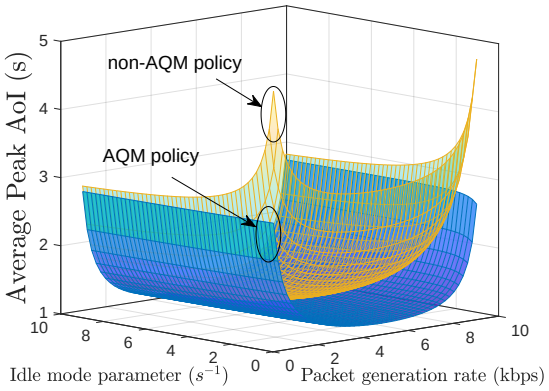

Fig. 4. The average PAoI under AQM policy and non-AQM policy over different packet generation rate λL_s and the idle mode parameter θ.

Then, according to Little's law [13], the average system delay of packet in the associated IoUT node's queue is obtained as:

$$\begin{aligned}\mathbb{E}[D_{NA}] &= \lambda^{-1}\sum_{k=1}^{+\infty} k\boldsymbol{\pi}_0\boldsymbol{R}^k\boldsymbol{e} \\ &= \lambda^{-1}\boldsymbol{\pi}_0(\boldsymbol{I}-\boldsymbol{R})^{-2}\boldsymbol{R}\boldsymbol{e}.\end{aligned} \tag{20}$$

According to Eq. (1), the expression of average PAoI for multiple vacation queue with non-AQM policy can be obtained as follows:

$$\begin{aligned}\mathbb{E}\left[A_{NA}^p\right] &= \mathbb{E}[G] + \mathbb{E}[D_{NA}] + \varrho \\ &= \lambda^{-1}\left[1 + \boldsymbol{\pi}_0(\boldsymbol{I}-\boldsymbol{R})^{-2}\boldsymbol{R}\boldsymbol{e}\right] + \varrho.\end{aligned} \tag{21}$$

According to Eqs. (5) and (19), the energy cost in the associated IoUT node relying on non-AQM policy is:

$$\mathcal{E}_{NA} = p_{NA,a} P_{tr} T_t = \frac{r_{21}}{1-\rho+r_{21}} P_{tr} T_t. \tag{22}$$

V. Numerical Results

In this section, we present numerical results to show the PAoI of the considered system in terms of different system parameters and policies, i.e., AQM, non-AQM and benchmark. The length of each packet is $L_s = 1.5$kb, the service rate of the IoUT node is $\mu = 10$, the capacity of the acoustic channel is $C = 15$kbps and the overall efficiency of the circuit is $\eta = 20\%$. The depth of IoUT node is $H = 100$m, the acoustic frequency of carrier is $f = 20$kHz, the transmission distance is $l = 1$km and the bandwidth of sub-channel is $B = 1$kHz.

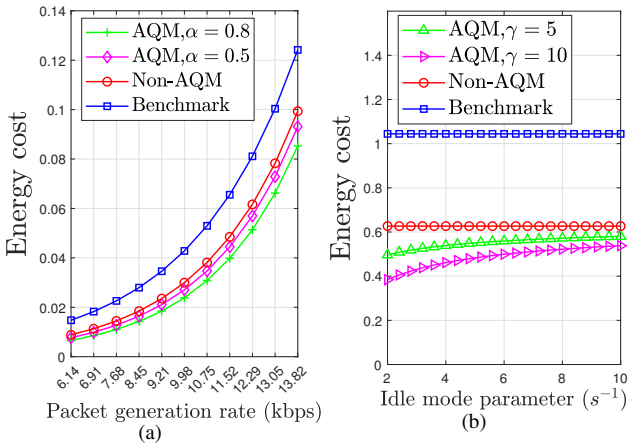

Fig. 5. The average energy cost of the IoUT node under three policies over different packet generation rate λL_s and the idle mode parameter θ.

Besides, an approximate value for underwater sound speed V_s is 1.5×10^3m/s [3]. Additionally, the amount of packets transmitted in our network simulator is 10^4.

Figs. 3(a) and 3(b) depict the average PAoI of the system considered as a function of packet generation rate (λL_s) for different idle mode parameter θ, the AQM rate γ and the discarding probability α, respectively. Specifically, simulation results are obtained through a network simulator, and closed-form results are analytical expressions. As the benchmark, IoUT nodes relying on age-optimal scheme generate and transmit data without the latency of idle period. Hence, it is obvious that such system can achieve the lowest peak AoI, which serves as the benchmark. When packet generation rate increases, the PAoI dramatically decreases firstly and increases after $\lambda L_s > 7.68$ kbps, because the excessive update interval and heavy system load aggravate the timeliness of packets. In Fig. 3(a), when the duration of the idle mode (θ^{-1}) increases, the average PAoI increases. This is because when θ decreases, the frequency of status update is reduced. In addition, the IoUT node relying on AQM is superior to non-AQM, because AQM processes the packets waiting a long term. Similarly, in Fig. 3(b), increasing the rate of AQM γ and the probability α contributes to the mitigation of the average PAoI.

Fig. 4 illustrates the average PAoI with different policies versus the idle mode parameter θ, and the packet generation rate, respectively. We set $\gamma = 10$ and $\alpha = 0.8$. As the figure shows, the average PAoI first decreases then increases with the growth of the packet generation rate, because the lack of update aggravates data timeliness when throughput is low. Then, the long system delay becomes the dominant factor with the excessive rate λL_s. However, the PAoI is not very sensitive to the idle mode parameter θ, because the larger γ and α frequently eliminate the packets with high PAoI.

Fig. 5(a) and (b) illustrate the energy cost of the IoUT node as a function of the packet generation rate λL_s and the idle mode parameter θ. It is obvious that the benchmark has the worst energy-efficiency, and the reason is instinctive. In underwater environment, the lack of sleep-scheduling causes excessive power dissipation. Fig. 5(a) shows that the energy cost increases with the growth of packet generation rate. Fig. 5(b) depicts the influence of the idle mode duration on the energy cost of the IoUT node. As it shows, with the growth of θ, if γ becomes large, the energy cost decreases, whereas when γ is small (i.e., $\gamma = 10$), the energy cost converges to a constant. It is noted that a larger sleep duration results in more packets transmitted and power dissipation. However, an arbitrarily large number cannot set γ or α because it leads to low network throughput.

VI. Conclusion

In this letter, we analytically evaluated the average PAoI and energy cost for an underwater information collection system relying on a pair of sleep-scheduling policies. Both the active mode and idle mode are considered to save energy consumption. Also, we derived closed-form expressions of average PAoI and energy cost in terms of both AQM and non-AQM policies, which were verified by sufficient numerical simulations. Simulation results indicate that to reduce the packets' PAoI, the IoUT node should choose an appropriate packet generation rate and compress packets having been waiting for a long time relying on AQM policy. Furthermore, the growth of the idle mode parameter mitigates energy cost and prolongs the lifetime of the system.

References

[1] S. Zhang, J. Liu, H. Guo, M. Qi, and N. Kato, "Envisioning device-to-device communications in 6G," *IEEE Network*, vol. 34, no. 3, pp. 86–91, May 2020.

[2] S. Guan, J. Wang, C. Jiang, R. Duan, Y. Ren, and T. Q. S. Quek, "Magicnet: The maritime giant cellular network," *IEEE Communications Magazine*, vol. 59, no. 3, pp. 117–123, Mar. 2021.

[3] Z. Fang, J. Wang, C. Jiang, Q. Zhang, and Y. Ren, "AoI inspired collaborative information collection for AUV assisted Internet of Underwater Things," *IEEE Internet of Things Journal*, vol. 8, no. 19, pp. 14 559–14 571, Jan. 2021.

[4] Z. Fang, J. Wang, Y. Ren, Z. Han, H. V. Poor, and L. Hanzo, "Age of information in energy harvesting aided massive multiple access networks," *IEEE Journal on Selected Areas in Communications, (10.1109/JSAC.2022.3143252)*, 2022.

[5] M. A. Abd-Elmagid, N. Pappas, and H. S. Dhillon, "On the role of age of information in the Internet of Things," *IEEE Communications Magazine*, vol. 57, no. 12, pp. 72–77, Dec. 2019.

[6] Y. Inoue, H. Masuyama, T. Takine, and T. Tanaka, "The stationary distribution of the age of information in FCFS single-server queues," in *IEEE International Symposium on Information Theory (ISIT)*, Aachen, Germany, 2017, pp. 571–575.

[7] S. Asvadi, S. Fardi, and F. Ashtiani, "Analysis of peak age of information in blocking and preemptive queueing policies in a HARQ-based wireless link," *IEEE Wireless Communications Letters*, vol. 9, no. 9, pp. 1338–1341, Apr. 2020.

[8] M. T. R. Khan, Y. Z. Jembre, S. H. Ahmed, J. Seo, and D. Kim, "Data freshness based AUV path planning for UWSN in the Internet of Underwater Things," in *IEEE Global Communications Conference (GLOBECOM)*, Hawaii, USA, 2019, pp. 1–6.

[9] N. Yaakob, I. Khalil, and M. Atiquzzaman, "Multi-objective optimization for selective packet discarding in wireless sensor network," *IET Wireless Sensor Systems*, vol. 5, no. 3, pp. 124–136, Jun. 2015.

[10] N. Tian and Z. G. Zhang, *Vacation Queueing Models: Theory and Applications*. Springer Science & Business Media, 2006, vol. 93.

[11] S. Dimou and A. Economou, "The single server queue with catastrophes and geometric reneging," *Methodology and Computing in Applied Probability*, vol. 15, no. 3, pp. 595–621, Aug. 2013.

[12] G. A. M. Jawad, A. K. M. Al-Qurabat, and A. K. Idrees, "Maximizing the underwater wireless sensor networks' lifespan using BTC and MNP5 compression techniques," *Annals of Telecommunications*, pp. 1–21, Jan. 2022.

[13] M. F. Neuts, *Matrix-geometric solutions in stochastic models: an algorithmic approach*. Courier Corporation, 1994.